CALCULATIONS OF ABSORPTION, ATTENUATION, AND BACKSCATTERING OF HAILSTONES AND THEIR POSSIBLE APPLICATIONS

Liu Jinli (刘锦丽)

Institute of Atmospheric Physics, Academia Sinica, Beijing

Received May 24, 1985

ABSTRACT

The absorption, attenuation, and backscattering of hailstones with various structures are investigated by the model calculations of four kinds of spherical hailstones: pure ice spheres, liquid water-coated ice spheres, spongy ice-coated ice spheres, and all spongy ice spheres. All the results for the wavelength 5.56 cm, including the radar reflectivity factor, absorption factor, and attenuation factor of hailstones with different size distributions are given and discussed in this paper. The possible applications of these characteristics in radar monitoring of hailstones are also discussed. It is shown that in certain conditions, a microwave radiometer simultaneously operating with a radar will be helpful to the identification of the hail-bearing area. Finally, the possible influence of hailfall area on the accuracy of the measurements of the rainfall distribution by using a radar-radiometer is simply discussed.

I. INTRODUCTION

Until recent years, radar monitoring of hailstorms is still one of the main subjects in nowcasting[1]. This is because that only the meteorological radar has the function of real-time monitoring and quantitative measurements of severe storms with high temporal and spatial resolutions. The physical basis of identifying hailstorms by conventional radar is the strong backscattering of hailstones. That means that, when strong echoes are found in some special area and with certain special morphology, one can identify it as hail-bearing area. This kind of method is useful in local hailstorm warning but usually with the limitation of local and personal experience. Since the 1970s other microwave characteristics of hailstones have been used for identifying hailstorms. One of them is to identify hailstorms with the dual-wavelength radar which is based on the differential reflectivities or differential attenuations of hailstones to these two radar wavelengths[2]. While in marginal success, this method requires one radar with attenuating wavelength (such as in X band) which limits the observation range. The other is to identify hailstorms with the polarization diversity radar which is based on the nonsphericity of hailstones which results in the differential reflectivities of hailstones to different polarizations[3]. But as we do not know the quantitative relationship between hailstone size and its nonsphericity, it seems that further information is needed for obtaining quantitative estimation of hailstorms.

In fact, in addition to the backscattering and attenuation of hailstones, the microwave absorption is also a significant characteristic to be investigated and used. In observations of quantitative rainfall distribution, a new scheme of combined radar-radiometer observation

has been suggested by Lü and Lin[4]. Primary field observation with this method showed that the accuracy of rainfall distribution was improved in comparison with that by using only radar. The reason is that the microwave radiometer observations supply the information on the microwave emission of raindrops. It is expected that the radar–radiometer system will be also useful to the identification of hailstorms.

The purpose of this paper is to systematically investigate backscattering, attenuation, and absorption of hailstones by using model calculations of spherical and layered-spherical hailstones, to analyze possible applications of these characteristics, especially the absorption to identifying hailstorms.

II. MODEL CALCULATIONS

In present model calculations, the Mie scattering formulation of hailstones of homogeneous spheres and two-layered spheres are used. From field observations of hailstone structure, we choose four kinds of spheres, i. e. pure ice sphere (hereinafter as PI), water-coated ice sphere (WI), spongy ice-coated sphere (SI), and all spongy ice sphere (AS) as model hailstones. The spongy ice is defined as homogeneous mixture of liquid and fine ice particles with different fraction of liquid water. The complex refractive indices of spongy ice are obviously different from pure ice or liquid water.

(1) *Formulae of model calculations*

All the formulae for Mie scattering of homogeneous sphere and two-layered sphere can be found in Refs. [5] and [6] (Kerker, 1969).

(2) *Complex refractive indices*

Ray's empirical formulae for the complex refractive indices of pure ice and liquid water are used in the present calculation[7] (Ray, 1972). The values used in present calculation are listed in Table 1. For spongy ice, the formula of Bohren et al. is used[8]. As Bohren et al. considered the spongy ice as fine ice particles immensed in liquid water, their formula gives more reasonable values. Values for the wavelength of 5.56 cm and the temperature of

Table 1. Complex Refractive Indices of Ice (m_1) and Water (m_2) for Different Wavelengths at 0°C

Wavelength (cm)	0.86	3.2	5.56	10.7
m_1 (ice)	$1.781-0.002400i$	$1.781-0.002404i$	$1.781-0.003606i$	$1.781-0.005764i$
m_2 (water)	$4.038-2.4535i$	$7.254-2.856i$	$8.406-2.192i$	$9.077-1.315i$

Table 2. Complex Refractive Indices of Spongy Ice with Different Values of f for Wavelength of 5.56 cm at 0°C

f	0.25	0.50	0.75	0.90
m	$6.9606-1.7559i$	$5.5268-1.2591i$	$3.9797-0.7398i$	$2.8820-0.2564i$

0°C are listed in Table 2.

(3) *Hailstone size distribution*

Very limited hailstone size distributions have been published. Most of the published size distributions have the exponential form, i. e.

$$N(D)=N_0\exp(-\lambda D), \tag{1}$$

where $N(D)$ is the spectral density of hailstone with the diameter of D; N_0 and λ are parameters characterizing the number concentration and the width of hailstone size distribution. Their values varied with the region and hailstorm type. Normalized to liquid water content, LWC=1 g/m^3, Douglas (1964)[9] gave the size distribution as

$$N(D)=31\exp(-3.09D). \tag{2}$$

Federer (1975)[10] gave the size distribution as

$$N(D)=12.1\exp(-4.02D). \tag{3}$$

A size distribution obtained from the collection of hailstones within a hailstorm in the north-western China had the form[11]

$$N(D)=1.07\exp(-1.25D). \tag{4}$$

The reflectivity Z_e, attenuation coefficient k_t, and absorption coefficient k_a are calculated by using the above size distributions, i. e.

$$Z_e=\int_{D_1}^{D_2}N(D)\sigma(D)dD, \tag{5}$$

$$k_t=0.4343\int_{D_1}^{D_2}N(D)Q_t(D)dD, \tag{6}$$

$$k_a=0.4343\int_{D_1}^{D_2}N(D)Q_a(D)dD, \tag{7}$$

where D_1 and D_2 are the minimum and maximum diameters of hailstones, respectively.

III. RESULTS

We have calculated the above characteristics (σ, Q_t, Q_a, Z_e, k_t, k_a) of hailstones for the wavelengths of 0.8, 3.2, 5.56, 10 cm. Only the results for the wavelength of 5.56 cm are discussed in this paper, as most of conventional radars in China are of the C band.

(1) *Backscattering, absorption, and attenuation of single hailstone*

For WI spheres, it is shown from model computations that, when the thickness of water shell is less than 10^{-4} cm, its σ, Q_t, and Q_a are almost equal to those for PI spheres of same size, respectively. With the increase of water shell thickness, σ, Q_t, and Q_a vary rather complicatedly. Until the water shell thickness is approximately equal to the diameter of the WI sphere, all the σ, Q_t, and Q_a are equal to values for the all-water spheres. Variations of σ, Q_t, and Q_a of PI and WI spheres with the sphere diameter D are partly shown in Fig. 1. It is seen from Fig. 1 that Q_t and Q_a increase monotonously for about 4 orders of magnitude with D of 0.6 to 5.0 cm, while the σ–D relation fluctuates. For $D>1$ cm, Q_t–D relation is relatively stable with weak variation of the thickness of water shell.

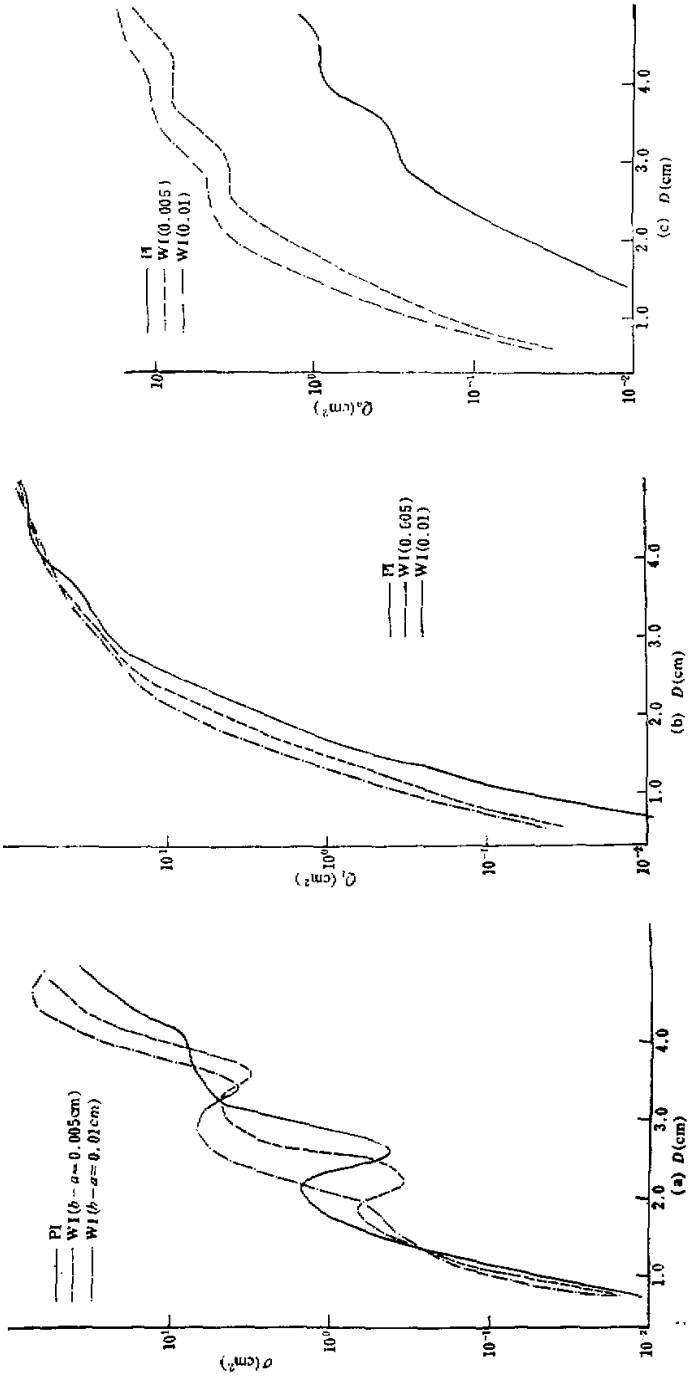

Fig. 1. Relations of σ–D, Q_t–D, and Q_a–D for PI and WI spheres.

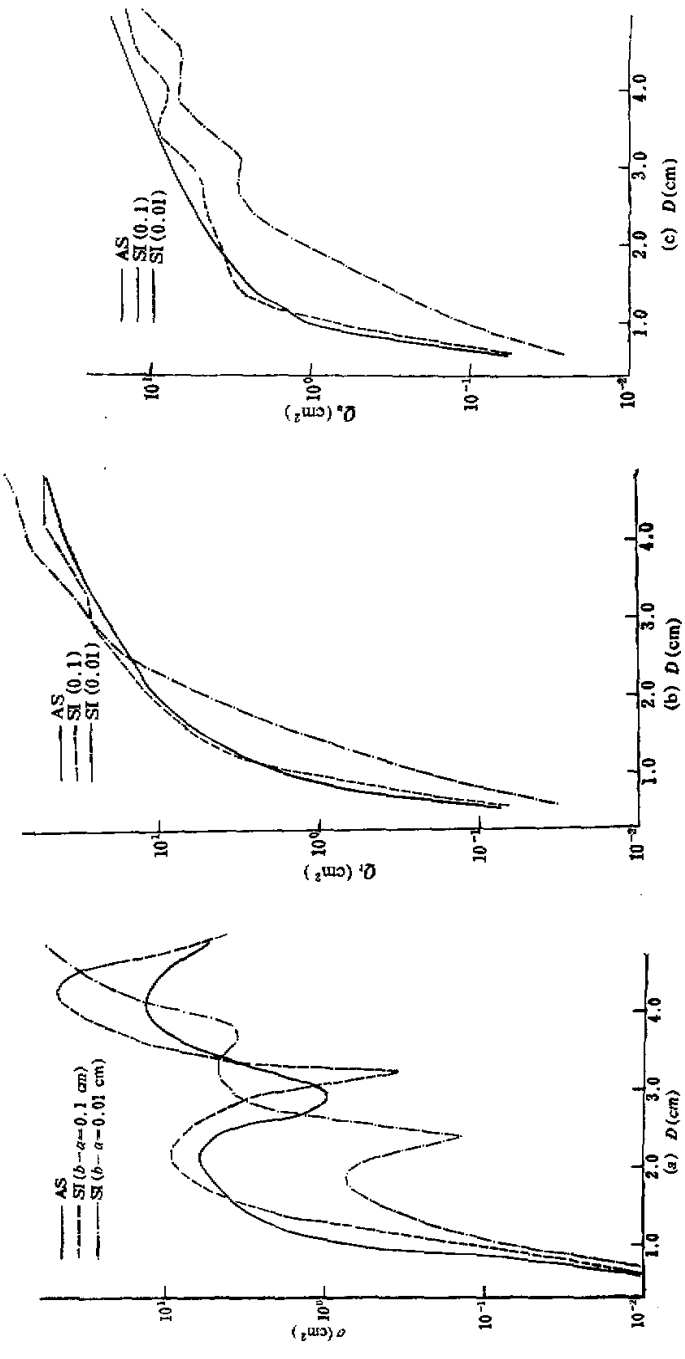

Fig. 2. As in Fig. 1, except for SI and AS spheres.

Fig. 2 shows part of the results for SI and AS spheres. The global trends of these curves are similar to results for PI and WI spheres. Q_t and Q_a increase monotonously with D, while σ fluctuates with D more strongly than σ–D relation for PI and WI spheres. This means that bigger hailstones may have lesser contribution to radar echo.

(2) *Relationship of σ, Q_t, and Q_a of single hailstone to its equivalent liquid water content (LWC)*

In physics of cloud and precipitation, LWC is a significant parameter. In order to investigate the relations between σ, Q_t and Q_a of single hailstone of different size and its

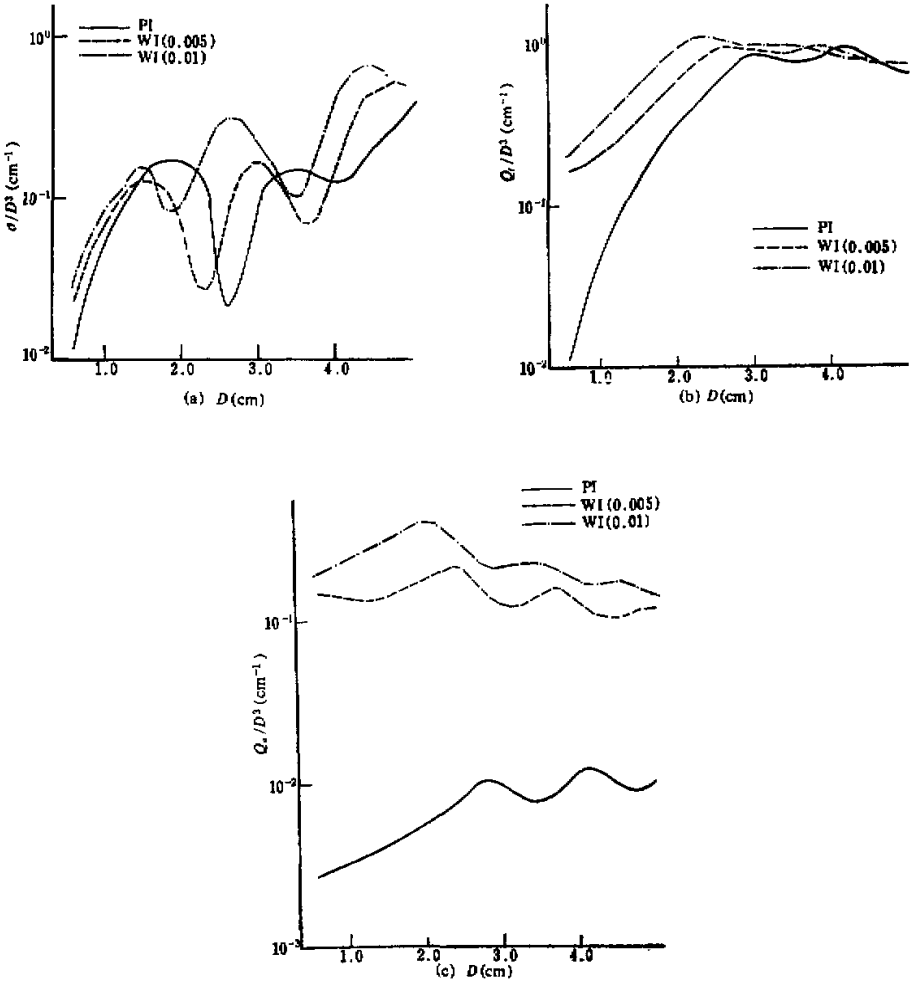

Fig. 3. Relations of σ/D^3–D, Q_t/D^3–D and Q_a/D^3–D (a,b,c respectively) for PI and WI spheres. Thickness of water shell are 5×10^{-3} and 0.01 cm, respectively.

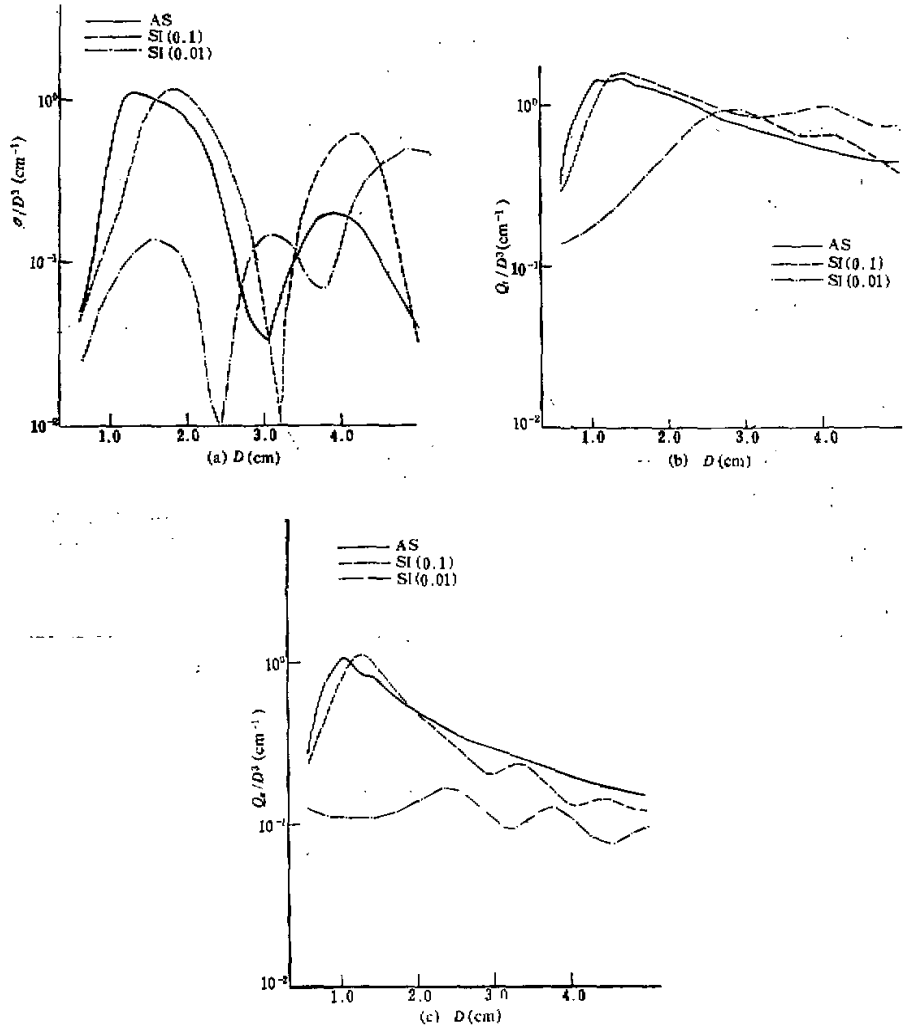

Fig. 4. As in Fig. 3, except for SI and AS spheres with the thickness of spongy ice shell being 0.01 and 0.1 cm respectively, and f=0.5.

equivalent LWC, we calculate the ratios of σ, Q_t, and Q_s to D^3. The possible variation of hailstone density is not considered here for simplicity. Figs. 3 and 4 show the relations of σ/D^3-D, Q_t/D^3-D, and Q_s/D^3-D for 4 types of model hailstones.

The following features can be seen from Figs. 3 and 4: 1) The relations of σ/D^3-D for all types of model hailstones have strong fluctuations with large amplitudes. For example, in the range of D=1.8—3.2 cm, the values of σ/D^3 of the SI sphere with 0.1 cm spongy ice

shell variate to 2 orders of magnitude. 2) The variations of Q_a/D^3 with D are much smaller than that of σ/D^3 with D. In the range of D of 0.6 to 5 cm, the total variation is less than a factor of 5. For PI and thin WI spheres, values of Q_a/D^3 are small and increase monotonously with D. For other types of model hailstones, Q_a/D^3 fluctuates with D and decreases slowly with D for certain larger D. That means that the Q_t/D^3 is relatively stable to the variation of hailstone size. 3) The variations of Q_t/D^3 with D for different model hailstones have similar trends. In the range of smaller D, Q_t/D^3 increases monotonously with D. For the range of $D>2.5$ cm (for thick SI spheres $D>1$ cm) it decreases slowly with D. Within the range of $2.0<D<5.0$ cm, $Q_t(D)/D^3$ has similar values for different model hailstones, the total variation is within a factor of 5. This means that Q_t/D^3 is relatively stable to the variation of hailstone size and structure. Therefore, this parameter will be suitable to the measurements of equivalent LWC of hailstones.

(3) *Relationship of Z_e, k_t, and k_a to polydispersed hailstones*

Z_e, k_t, and k_a are calculated for the "exponential" size distribution of polydispersed hailstones as the function of D_{max}. The actual size distribution in present calculations is

$$N(D)=1.07\exp(-1.25D), \tag{8}$$

where D in cm, $N(D)$ in m^{-3} cm^{-1}.

Figs. 5, 6, and 7 show the Z_e-D, k_t-D, and k_a-D relations of the exponential size distribution for different model hailstones. These are part of our calculated results. The following features of these relations can be drawn from the model calculations: 1) All these relations for PI and thin WI spheres are approximately consistent with each other. Similarly, all these relations for AS and thick SI spheres ($b-a=0.1$ cm) are approximately consistent as well. 2) For WI spheres, when the thickness of water shell increases from

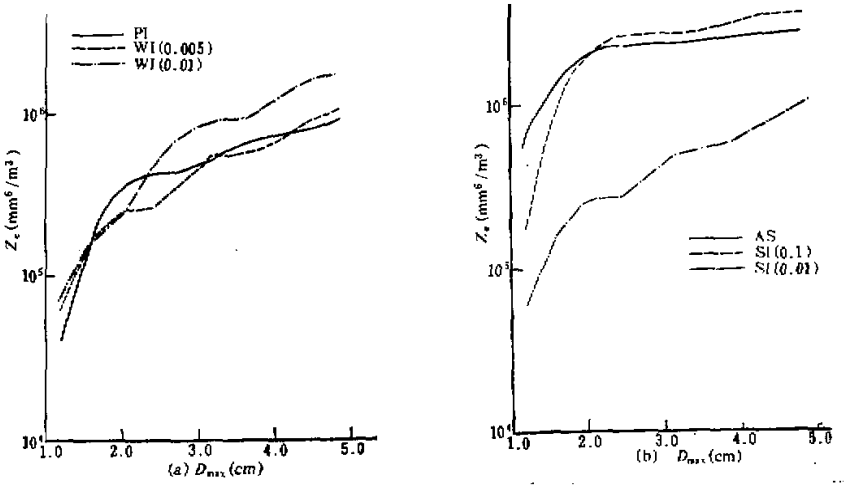

Fig. 5. Z_e-D_{max} relation of the exponential size distribution (8) for different model hailstones.PI (a) for and WI spheres ($b-a=$ 0.005, 0.01 cm, respectively), (b) for SI and AS spheres ($b-a=$ 0.005, 0.01, 0.1, 0.2 cm, respectively).

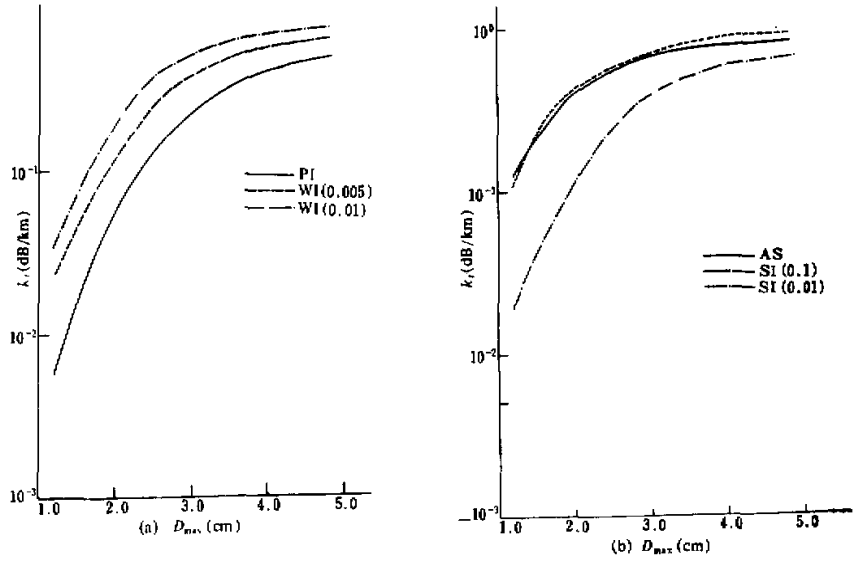

Fig. 6. Same as in Fig. 5, except for k_j–D_{max} relation.

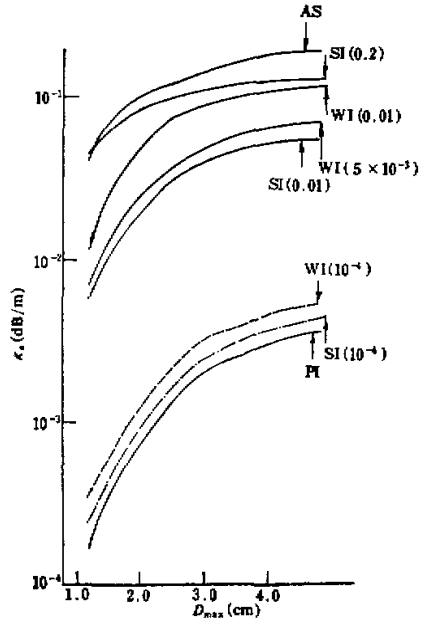

Fig. 7. k_a–D_{max} relation, for both WI spheres ($b-a$=0.0001, 0.005, 0.01 cm, respectively) and SI spheres ($b-a$=0.0001, 0.01, 0.2 cm, respectively).

10^{-4} cm to 0.01 cm, the values of Z_e and k_t variate very slowly, within a factor of 2 in comparison with the corresponding values for PI spheres. For thin SI ($b-a<0.01$ cm), the variations of Z_e and k_t with D are approximately equal to those for corresponding WI spheres. However, for thick SI spheres, the values of Z_e are ten times larger than those for thin SI spheres at same D, and those of k_t are five times larger. This means that the values of Z_e and k_t are more sensitive to the thickness of the shell than the difference of shell structure (spongy ice or water shell). 3) For PI and very thin WI spheres, the values of k_a are very small and consistent with each other. However, as the thickness of shell is larger than 10^{-4} cm, the values of k_a are several dozen times larger than those for PI and thin WI spheres and insensitive to the thickness and structure of the shell.

IV. POSSIBLE APPLICATIONS

Based on the above model calculations, we shall simply discuss some possible applications in hailstorm identification and related problems. The values of Z_e, k_t, and k_a for different model hailstones with the size distribution of (8) and typical rain of different rainfall rates are listed in Table 3, where the first raw lists the equivalent LWC. In Table 4, values of Z_e, k_t, and k_a are listed for model hailstones with the size distribution of (2) for 2 g m^{-3} of equivalent LWC. Those values for rain in Tables 3 and 4 are obtained from the regressive relations of Z_e, k_t, and k_a with the LWC of the rainfall for Beijing mixed-type rain. These regressive relations represent the typical situation of strong showery rain in Beijing.

For convenience of discussion, the simplified meteorological radar equation and the equation for microwave radiometer observation are written as follows:

$$P(R)=C_A|K|^2R^{-2}Z_e(R)\exp\left(-2\int_0^R k_t(R')dR'\right), \tag{9}$$

$$T_B=\int_0^\infty T(R)k_a(R)\exp\left(-\int_0^R k_t(R')dR'\right)dR, \tag{10}$$

where R is distance, C is radar constant, and $T(R)$ is air (as well as cloud and rain) temperature (K).

It can be seen from Tables 3 and 4 that obvious differences exist among the values of corresponding characteristics for different model hailstones and shower rainfall. Some of these differences are favorite to the identification of hailstorms. Also these differences will affect the accuracy of radar measurements of rainfall distribution.

(1) Identification of the forming area of primitive hailstones within strong convective storms. Radar observations show that primitive hailstones are formed in the mid-upper portion of strong convective clouds where the air temperature is below 0°C. So it is believed that hailstones in this layer consist of PI or very thin WI spheres. It can be seen that for the same equivalent LWC, the values of Z_e for PI and very thin WI spheres are about ten times larger than those for showery rain. On the contrary, the values of k_a for PI and thin WI spheres are about ten times smaller than those for showery rain. Therefore, it is expected that when observations are made to the strong convective clouds with a radar and a microwave radiometer, those areas with strong radar reflectivities and low microwave brightness temperature will be identified as hailstone forming areas.

Table 3. Z_e(mm^6 m^{-3}), k_t and k_a (dB km^{-1}) for Model Hailstones of (8) and Showery Rainfall

		1 g m^{-3}			2 g m^{-3}			4 g m^{-3}		
		Z_e	k_t	k_a	Z_e	k_t	k_a	Z_e	k_t	k_a
Rain		2.49×10^4	6.37×10^{-3}	5.97×10^{-2}	8.09×10^4	1.56×10^{-1}	1.49×10^{-1}	2.63×10^5	3.81×10^{-1}	3.61×10^{-1}
PI		8.37×10^5	5.03×10^{-1}	3.49×10^{-3}	1.67×10^6	1.01	6.90×10^{-3}	3.35×10^6	1.79	1.40×10^{-2}
WI	10^{-4}(cm)	8.29×10^5	5.06×10^{-1}	5.31×10^{-3}	1.66×10^6	1.01	1.06×10^{-2}	3.32×10^6	2.01	2.12×10^{-2}
	5×10^{-3}	8.84×10^5	6.57×10^{-1}	6.86×10^{-2}	1.77×10^6	1.31	1.37×10^{-1}	3.54×10^6	2.63	2.74×10^{-1}
	10^{-2}	1.57×10^6	7.80×10^{-1}	1.19×10^{-1}	3.14×10^6	1.56	2.38×10^{-1}	6.28×10^6	3.12	4.76×10^{-1}
SI	10^{-4}(cm)	8.33×10^5	5.04×10^{-1}	4.09×10^{-3}	1.67×10^6	1.01	8.18×10^{-3}	3.33×10^6	2.02	1.64×10^{-2}
	10^{-2}	8.14×10^5	6.32×10^{-1}	5.57×10^{-2}	1.63×10^6	1.26	1.11×10^{-1}	3.26×10^6	2.53	2.23×10^{-1}
	10^{-1}	3.60×10^6	9.22×10^{-1}	1.77×10^{-1}	7.20×10^6	1.84	3.54×10^{-1}	1.44×10^7	3.69	7.08×10^{-1}
	2×10^{-1}	4.34×10^5	8.35×10^{-1}	1.30×10^{-1}	8.68×10^5	1.67	2.60×10^{-1}	1.73×10^7	3.34	5.20×10^{-1}
AS (f=0.50)		2.73×10^6	8.92×10^{-1}	1.91×10^{-1}	5.46×10^6	1.66	3.82×10^{-1}	1.09×10^7	3.33	7.64×10^{-1}

Table 4. Z_e, k_t and k_a for Model Hailstones of (2) and Showery Rainfall for LWC=2 g m^{-3}

		Z_e (mm^6 m^{-3})	k_t (dB km^{-1})	k_a (dB km^{-1})
Rain		8.09×10^4	1.56×10^{-1}	1.49×10^{-1}
PI		1.10×10^6	2.52×10^{-1}	7.14×10^{-3}
WI	10^{-4}(cm)	1.10×10^6	2.60×10^{-1}	1.39×10^{-2}
	5×10^{-3}	1.03×10^6	5.78×10^{-1}	2.58×10^{-1}
	10^{-2}	1.28×10^6	8.50×10^{-1}	4.50×10^{-1}
SI	10^{-4}(cm)	1.10×10^6	2.56×10^{-1}	9.78×10^{-3}
	5×10^{-3}	1.04×10^6	3.96×10^{-1}	1.19×10^{-1}
	10^{-1}	1.03×10^6	5.18×10^{-1}	2.10×10^{-1}
	2×10^{-1}	9.08×10^5	1.74	9.40×10^{-1}
AS (f=0.5)		7.52×10^6	1.84	1.11

(2) For near ground hailstones which consist mainly of melting ice (WI, SI, and AS spheres), their reflectivity is 1—2 orders of magnitudes larger than that for showery rainfall of the same LWC, while its attenuation k_t is 1—10 times larger. As for its absorption k_a, in most cases the k_a of melting hailstones is approximate to that of showery rain with the same LWC, with only exception that the k_a for SI spheres with shell thickness of 0.2 cm is about 6—7 times larger than that for showery rain. In this situation the microwave brightness temperature observed with a microwave radiometer to wet hailstones will be of no major difference in comparison to that to showery rain. Extra strong radar echo of special shape(s) will be a main indication of wet hailstones. The information of microwave

brightness temperature of wet hailstones should be further investigated.

As hailstone cells are usually accompanied with rain cells in the line of sight of radar and microwave radiometer, we need to investigate a combined scheme of remote sensing of rain and hailstones by using a combined radar–radiometer system.

REFERENCES

[1] Radar Meteorology Group, Institute of Atmospheric Physics (1981), *Radar Monitoring of Hailstorms*, Science Press, Beijing, 220 pp. (in Chinese).

[2] Eccles, P. J. and Atlas, D. (1970), A new method of hail detection by dual-wavelength radar, in *14th Radar Met. Conf.*, pp. 1—6.

[3] Seliga, T. A. et al. (1981), Hydrometeor characteristics in the May 2, 1979 squall line in central Oklahoma as obtained from radar differential reflectivity measurement during SESAME, in *20th Radar Met. Conf.*, pp. 561—566.

[4] Lü Daren and Lin Hai (1980), Comparison of radar and microwave radiometer in precipitation measurements and their combined use, *Scientia Atmospherica Sinica*, **4**: 30—39.

[5] Deirmendjian, D. (1969), *Electromagnetic Scattering by Polydispersion*, Am. Elsevier, New York, 290 pp.

[6] Kerker, M. (1969), *The Scattering of Light and Other Electromagnetic Radiation*, Academic Press, New York, 666 pp.

[7] Ray, P. S. (1972), Broadband complex refractive indexes of ice and water, *Appl. Opt.*, **11**: 1836—1845.

[8] Bohren, C. F. and Battan L. J. (1980), Radar backscattering by inhomogeneous precipitation particles, *J. Atmos. Sci.*, **37**: 1821—1827.

[9] Douglas, R. H. (1964), Hail size distribution, Preprints *11th Wea. Radar Conf.*, pp. 146—149.

[10] Federer, B. and Waldvogel, A. (1975), Hail and raindrop size distribution from a Swiss multicell storm. *J. Appl. Met.*, **14**: 91—97.

[11] Xu Jialiu (1979), *Microphysics and Forming Mechanism of Hailstones*, Agricultural Press, Beijing, 232 pp. (in Chinese).

[12] Microwave Remote Sensing Group, Institute of Atmospheric Physics (1982), *Microwave Propagation and Radiation Characteristics of Clear, Cloudy, and Rainy Atmosphere Over China*, National Defense Industry Press, Beijing, 161 pp. (in Chinese).